

reduction of the double bond (approaching complete exchange of D for H in some cases); and (3) each substrate gave the perdeuterated isotopomer as the major product.

The observation that extensively polydeuterated cycloalkanes can be produced from cycloolefins with H₂ as the reductant is remarkable and potentially useful in the synthesis of isotopically labeled compounds. The ability to incorporate deuterium into organic compounds by the metal-catalyzed reduction of olefins with H₂ and D₂O/THF avoids the need for D₂. In addition, this technique should be applicable to the incorporation of tritium into organic compounds.

Previous studies of the hydrogenation of olefins in protic solvents showed that surface alkyls on platinum rapidly undergo isotopic exchange of hydrogen with H• (D•) and that the product alkanes contain the isotope from the solvent (ROH or ROD).⁷⁻¹³ Our results demonstrate that by working under mass-transport-limited conditions, isotopic exchange can be made more extensive than in these earlier reports. The exchange undoubtedly requires exchange between H• (D•) and the OH (OD) group of the solvent (eq 2). The mechanism of the exchange shown in eq 2 is not well established, although several mechanisms have been proposed.¹⁰⁻¹⁶



Because the exchange of H/D between the surface of platinum and the protic solvent is, under the conditions used here, faster than the conversion of surface alkyls to alkanes, the content of deuterium in the product alkanes provides a valuable mechanistic tool: a measure of the rate of exchange (and thus of C-H bond activation) of the surface alkyls relative to the rate of their reductive elimination as alkanes. Comparison of the ratio d_{av}/d_{2n} from the reduction of a series of cycloalkenes demonstrates the utility of this approach (Figure 2). These data indicate that the rates of C-H activation (relative to the rates of reductive elimination) of surface cycloalkyls decrease from cyclodecyl- to cyclohexyl.

The value of d_{av}/d_{2n} correlates with the strain energy of the product cycloalkanes ($r = 0.95$).¹⁷⁻¹⁹ Thus, as the cycloalkane is varied from one having low strain energy to one having high strain energy, the transition state for reductive elimination increases in energy relative to that for isotopic exchange. The two simple limiting hypotheses rationalizing this inference are that strain is *relieved* in the transition state for isotopic exchange (C-H activation) or that strain is *concentrated* in the transition state for reductive elimination.²¹ We emphasize that ΔG^\ddagger for reductive

elimination by reaction of R• with H₂ is dominated by the free energy term describing generation of H• by a mass-transport-limited process. We therefore hypothesize that the correlation in Figure 2 reflects primarily structure-dependent differences in rates of C-H activation.

The heterogeneous polydeuteration of hydrocarbons probably involves some combination of $\alpha\alpha$ -activation, $\alpha\beta$ -activation, and π -allyl formation.²² The differences in strain energies between the transition states leading to these intermediates and the transition states leading to the cycloalkane products should correlate with d_{av}/d_{2n} . Calculating strain energies for the intermediates is, however, too complicated to be approached through realistic models of surface species.²³ To date, our efforts to obtain a correlation between the experimental values of d_{av}/d_{2n} and relative strain energies calculated for simple models of surface intermediates have not been successful.

Acknowledgment. We thank our colleagues John Burns and Watson Lees for assistance with the force field calculations.

(21) There are several reports in the literature of correlations between the strain energy and the rates of reaction of functionalized cycloalkanes. For recent examples, see: Schneider, H. J.; Thomas, F. *J. Am. Chem. Soc.* **1980**, *102*, 1424-1425. Schneider, H. J.; Schmidt, G.; Thomas, F. *J. Am. Chem. Soc.* **1983**, *105*, 3556-3563.

(22) Lebrilla, C. B.; Maier, W. F. *J. Am. Chem. Soc.* **1986**, *108*, 1606-1616 and references therein.

(23) The hydrocarbon species believed to exist on the surfaces of noble metal catalysts were summarized recently: Cogen, J. M.; Maier, W. F. *J. Am. Chem. Soc.* **1986**, *108*, 7752-7762 and ref 22 of this paper.

Four-Dimensional [¹³C, ¹H, ¹³C, ¹H] HMQC-NOE-HMQC NMR Spectroscopy: Resolving Tertiary NOE Distance Constraints in the Spectra of Larger Proteins

Erik R. P. Zuiderweg,* Andrew M. Petros, Stephen W. Fesik, and Edward T. Olejniczak

Pharmaceutical Discovery Division, Abbott Laboratories
D47G, AP9, Abbott Park, Illinois 60064

Received September 27, 1990

Three-dimensional (3D) heteronuclear-resolved nuclear Overhauser effect (NOE) NMR spectroscopy is a powerful tool to improve the resolution of NOE spectra of medium-sized proteins (MW <25 kDa) that are isotopically labeled.¹ However, even with 3D NMR methods it is difficult to resolve and unambiguously identify many of the NOE cross peaks. Therefore, a further increase in dimensionality of the NMR experiments is necessary. Recently, the first four-dimensional (4D) NMR spectrum appeared,² where amide-aliphatic proton NOEs of interleukin 1- β were edited with respect to two different heteronuclei.

Here we demonstrate a four-dimensional NMR experiment (4D [¹³C, ¹H, ¹³C, ¹H] HMQC-NOE-HMQC, see panel A of Figure 1), carried out with ¹³C-labeled T4-lysozyme (MW 19.7 kDa), in which both dimensions of ¹H-¹H NOE cross peaks between aliphatic and/or aromatic protons are edited by the frequencies of both attached ¹³C nuclei.³ The resulting four-dimensional

(7) Eidinoff, M. L.; Knoll, J. E.; Fukushima, D. K.; Gallagher, T. F. *J. Am. Chem. Soc.* **1952**, *74*, 5280-5284.

(8) Phillipson, J. J.; Burwell, R. L., Jr. *J. Am. Chem. Soc.* **1970**, *92*, 6125-6133.

(9) Trahanovsky, W. S.; Bohlen, D. H. *J. Org. Chem.* **1972**, *37*, 2192-2197.

(10) Shimazu, K.; Kita, H. *J. Chem. Soc., Faraday Trans. 1* **1985**, *81*, 175-183.

(11) Fujikawa, K.; Kita, H.; Sato, S. *J. Chem. Soc., Faraday Trans. 1* **1981**, *77*, 3055-3071.

(12) Fujikawa, K.; Kita, H.; Miyahara, K.; Sato, S. *J. Chem. Soc., Faraday Trans. 1* **1975**, *71*, 1573-1581.

(13) Kita, H. *Isr. J. Chem.* **1979**, *18*, 152-161.

(14) Sagert, N. H.; Pouteau, R. M. L. *Can. J. Chem.* **1974**, *52*, 2960-2967.

(15) Miyamoto, S.-I.; Sakka, T.; Iwasaki, M. *Can. J. Chem.* **1989**, *67*, 857-861.

(16) Rolston, J. H.; Goodale, J. W. *Can. J. Chem.* **1972**, *50*, 1900-1906.

(17) The maximum possible content of deuterium in a cycloalkane is d_{2n} .

(18) We calculated strain energies for the lowest energy conformations of the cycloalkanes given in the following: Burkert, U.; Allinger, N. L. *Molecular Mechanics*; ACS Monograph 177; American Chemical Society: Washington, DC 1982; pp 89-108 (for C₅-C₁₂). Anet, F. A. L.; Rawdah, T. N. *J. Am. Chem. Soc.* **1978**, *100*, 7810-7814 (for C₁₅). The strain energies for these conformations were calculated with MacroModel V2.0 using the MM2(85) parameter set: Still, W. C.; Mohamadi, F.; Richards, N. G. J.; Guida, W. C.; Liskamp, R.; Lipton, M.; Caufield, C.; Chang, G.; Hendrickson, T. *MacroModel V2.0*; Dept. of Chemistry, Columbia University: New York, NY.

(19) The strain energies shown in Figure 2 were obtained by standard modification of the values given by force field calculations ($SE = SE_{MM2} - SE_{strainless}$).²⁰ The values for $SE_{strainless}$ were empirically determined to be $n \times 0.65$ kcal/mol for a given cycloalkane (C_nH_{2n}).

(20) See, for example: DeTar, D. F.; Tenpas, C. J. *J. Org. Chem.* **1976**, *41*, 2009-2013.

(1) (a) Fesik, S. W.; Zuiderweg, E. R. P. *J. Magn. Reson.* **1988**, *78*, 588-593. (b) Marion, D.; Kay, L. E.; Sparks, S. W.; Torchia, D. A.; Bax, A. *J. Am. Chem. Soc.* **1989**, *111*, 1515-1517. (c) Zuiderweg, E. R. P.; Fesik, S. W. *Biochemistry* **1989**, *28*, 2387-2391. (d) Ikura, M.; Kay, L. E.; Tschudin, R.; Bax, A. *J. Magn. Reson.* **1990**, *86*, 204-209. (e) Zuiderweg, E. R. P.; McIntosh, L. P.; Dahlquist, F. W.; Fesik, S. W. *J. Magn. Reson.* **1990**, *86*, 210-216.

(2) Kay, L. E.; Clore, G. M.; Bax, A.; Gronenborn, A. M. *Science* **1990**, *249*, 411-414.

(3) The 4D spectrum appears as a series (f_1) of 3D spectra ($f_2/f_3/f_4$). Each 3D spectrum corresponds to a subset of the 4D data set in which only those f_2 protons appear that are attached to carbons resonating at a particular frequency range of f_1 . Every 3D spectrum contains a set (f_3) of (f_3/f_4) ¹H-¹H NOESY planes. These planes correspond to a subset of the 3D data in which only those f_4 protons appear that are attached to carbons resonating at a particular frequency range of f_3 (see also Figure 1 of ref 2).

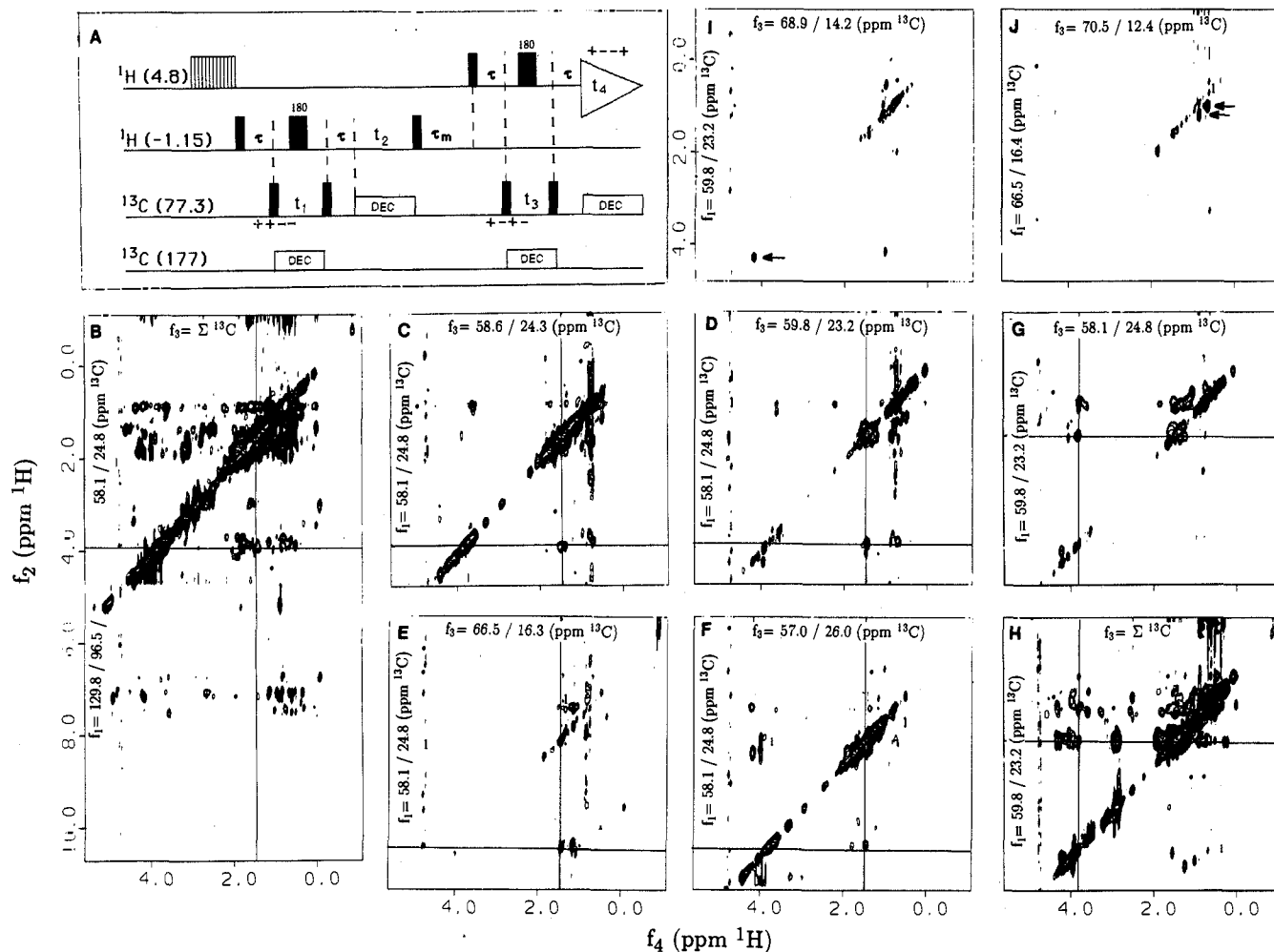


Figure 1. Panel A: Pulse sequence of the 4D $[^{13}\text{C}, ^1\text{H}, ^{13}\text{C}, ^1\text{H}]$ HMQC-NOE-HMQC experiment. Carrier frequencies are indicated at the left in ppm; τ is the evolution time for heteronuclear antiphase magnetization; τ_M is the NOE mixing time. The phase cycle is indicated with + and - in the figure. The proton carrier frequency is at the high-field side of the spectrum during the first part of the experiment to avoid quadrature images in f_2 . Panels C-G, I, and J: A selection of (f_2, f_4) ^1H - ^1H cross sections through the 4D NOESY experiment, carried out with 3.8 mM ^{13}C -labeled T4-lysozyme (19.7 kDa) in $^2\text{H}_2\text{O}$, pH 4.5, 20 $^\circ\text{C}$, using a Bruker AM-500 NMR spectrometer equipped with a process-controller interrupter (Tschudin Associates, Kensington, MD), and two additional channels, each consisting of a synthesizer, a Bruker BSV-3 amplifier, and a GARP⁷ decoupler modulator (Tschudin Associates, Kensington, MD). In each panel, the f_1 chemical shift (which edits f_2) is given at the vertical axis, while the f_3 chemical shift (which edits f_4) is given at the horizontal axis. Projections of all the planes f_3 at a particular f_1 frequency, corresponding to planes from a 3D HMQC-NOESY experiment,¹⁶ are given in panels B and H. Experimental parameters were as follows: spectral width SW in f_1 (SW(f_1)), 36.14 ppm; SW(f_2), 11.9 ppm; SW(f_3), 36.14 ppm; SW(f_4), 17.85 ppm; number of increments in t_1 ($N(t_1)$) 36 real points; $N(t_2)$, 128 real points; $N(t_3)$, 32 real points; $N(t_4)$, 2048 TPP1 points; GARP decoupling at 77.3 ppm, 3.57 kHz rf; GARP decoupling at 177 ppm (carbonyl^{1d}), 0.28 kHz; τ , 3.5 ms; τ_M , 100 ms; relaxation delay, 1 s. The initial delays in both carbon dimensions were set to $1/2$ dwell in order to obtain phase inversion of the folded resonances.^{1d} The data was acquired as a series (t_1) of a series (t_2) of (t_2, t_4) NOESY spectra with four scans/increment; six dummy scans were given before each NOESY experiment of 128 increments. Total acquisition time was 216 h. The sensitivity of the 4D NOE experiment was found to be comparable to that of a 2D NOE spectrum acquired in an overnight run. The data was processed in 62 h on a Silicon Graphics 4D-220 computer using in-house-written software. The t_1 , t_2 , and t_3 interferograms were extended by linear prediction⁸ to 44, 160, and 40 points and were apodized by Hamming windows shifted by 45° , 60° , and 45° , respectively. t_4 was apodized by a Lorentz-Gauss transformation. Base-line corrections were applied in f_2 and f_4 . Only the f_4 region from 5.6 to -1.1 ppm was processed in t_1 , t_2 , and t_3 . The final data matrix size was (f_1, f_2, f_3, f_4) $64 \times 256 \times 64 \times 384$ points. The digital resolution was 71, 23, 71, and 8.7 Hz/point in f_1 , f_2 , f_3 , and f_4 , respectively.

spreading of this most crowded region of protein NMR spectra is extremely important, since the majority of the NOEs that define the tertiary structure resonate here. The experiment provides the means to improve the quality of NMR solution structures by allowing unambiguous identification of more of those NOEs and opens the possibility of studying larger molecules with broader NMR lines because of a dramatic improvement in resolution as compared to 3D NMR.

Panel B of Figure 1 shows a superimposition of planes from the 4D NOE spectrum, equivalent to a single plane taken out of a 3D ^{13}C -resolved HMQC-NOESY spectrum.¹⁶ In 4D NOE, this plane is further edited by the second ^{13}C frequency (f_3). Panels C-F show that four NOEs resonate at approximately the same ^1H f_2 and f_4 frequencies (cross hairs). These NOEs are not resolved in the plane shown in panel B of a 3D spectrum; neither are they in the diagonally related planes (except for the peak in

panel F). The overlap is shown for the cross peaks in panel 1G, which are symmetry related to the peaks in panel 1D. In 3D ^{13}C -resolved NOE spectroscopy these peaks would resonate together with many more in a single plane, as illustrated in the projection at this frequency in panel H. Thus, the increase in resolution of 4D NOE spectroscopy as compared to 3D NOE spectroscopy is appreciated by comparing panel D (4D) with panel B (3D) and panel G (4D) with panel H (3D). Clear identification of the overlapping cross peaks is obtained in the 4D experiment from the four frequency coordinates, provided that the ^1H and ^{13}C assignments (e.g., from ^{13}C - ^{13}C transfer experiments⁴) are known. This is not the case in 3D ^{13}C -resolved NOE spectroscopy,

(4) (a) Fesik, S. W.; Eaton, H. L.; Olejniczak, E. T.; Zuiderweg, E. R. P.; McIntosh, L. P.; Dahlquist, F. W. *J. Am. Chem. Soc.* **1990**, *112*, 886-888. (b) Kay, L. E.; Ikura, M.; Bax, A. *J. Am. Chem. Soc.* **1990**, *112*, 888-889.

where, even if two overlapping cross peaks are resolved, they cannot be unambiguously assigned to either of two possible proton-proton NOEs. Another particularly useful feature of the 4D experiment is the possibility of identifying NOEs between protons with identical chemical shifts. Consider the two cross peaks originating from a NOE between the protons HA and HB in the molecular fragment CA-HA...HB-CB. When $\Omega_{HB} = \Omega_{HA} = \Omega_X$, the cross peaks between these protons will resonate on the diagonal in 2D and 3D NOE spectroscopy. In the 4D experiment, the cross peaks are found at the coordinates (f_1, f_2, f_3, f_4) ($\Omega_{CA}, \Omega_X, \Omega_{CB}, \Omega_X$) and $(\Omega_{CB}, \Omega_X, \Omega_{CA}, \Omega_X)$ distinct from the diagonal peaks at $(\Omega_{CA}, \Omega_X, \Omega_{CA}, \Omega_X)$ (HA) and $(\Omega_{CB}, \Omega_X, \Omega_{CB}, \Omega_X)$ (HB), provided that $\Omega_{CA} \neq \Omega_{CB}$.⁵ An example of this case is given in panel I of Figure 1, where a strong cross peak (arrow) is seen on the virtual diagonal,⁶ showing an NOE between two protons that have identical chemical shifts but are attached to carbons with different shifts. Many methyl-methyl NOE cross peaks resonate close to or at the diagonal in 2D and 3D spectroscopy. Such peaks are readily identified in the 4D experiment (panel J), which is extremely important for the determination of the 3D structure of the hydrophobic core of proteins, where many methyl-methyl contacts occur.

In summary, it is demonstrated here that four-dimensional ¹³C-resolved NOE spectroscopy yields spectra of greatly enhanced resolution. This method allows for the study of larger proteins by NMR and will contribute to the improvement of the quality of tertiary structures derived from NMR data. The same four-dimensional "double chemical shift labeling" method can be applied to H-C-C-H experiments⁴ and to ¹⁵N-resolved NOE spectra.^{1a-c}

Acknowledgment. Drs. Lawrence P. McIntosh and Frederick W. Dahlquist are acknowledged for the preparation of the isotopically labeled sample of T4-lysozyme.

(5) Note that inversion symmetry exists in the 4D data which can be exploited to enhance the S/N ratio and/or to reduce the final data size.

(6) Residual diagonal signals are observed in the "nondiagonal" planes due to ridges which were insufficiently suppressed. However, true cross peaks could be distinguished from the ridges by their symmetry relationships.

(7) Shaka, A. J.; Barker, P. B.; Freeman, R. J. *Magn. Reson.* **1985**, *64*, 547-552.

(8) Olejniczak, E. T.; Eaton, H. L. *J. Magn. Reson.* **1990**, *87*, 628-632.

Characterization of High-Nuclearity Platinum Carbonyl Cluster Anions by ²⁵²Cf-Plasma Desorption Mass Spectrometry: Formation of Gas-Phase $[\text{Pt}_{26}(\text{CO})_x]_n$ Monocharged Ion Oligomers ($n = 1-20$) from Solid-State $[\text{Pt}_{26}(\text{CO})_{32}]^{2-}$ Dianions

Catherine J. McNeal,*^{1a} Janita M. Hughes,^{1a}
Gregory J. Lewis,^{1b} and Lawrence F. Dahl*^{1b}

Department of Chemistry, Texas A&M University
College Station, Texas 77843

Department of Chemistry, University of Wisconsin—Madison
Madison, Wisconsin 53706

Received August 1, 1990

Revised Manuscript Received October 18, 1990

The great potential of mass spectrometry for characterizing giant-sized metal clusters was first demonstrated by Fackler, McNeal, Winpenny, and Pignolet,² who used ²⁵²Cf-plasma desorption mass spectrometry (PDMS)³ to analyze the Schmid

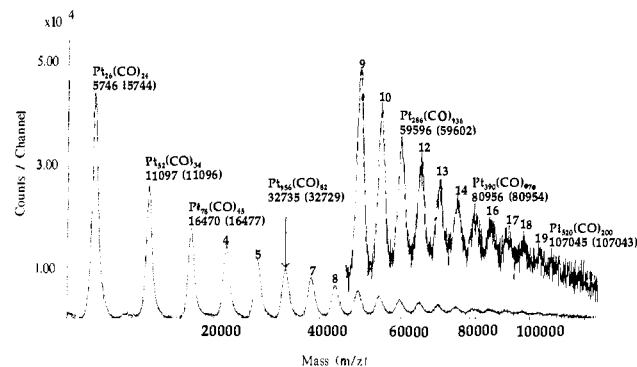


Figure 1. ²⁵²Cf plasma desorption positive-ion mass spectrum of $[\text{Pt}_{26}(\text{CO})_{32}]^{2-}$. The major peak in both the positive- and negative-ion mass spectra is due to a monocharged parent ion Pt_{26} core; its peak maximum in this spectrum at m/z 5746 corresponds most closely to the partially decarbonylated $[\text{Pt}_{26}(\text{CO})_{24}]^+$ ion (5744 u). The other high-mass peaks are readily attributed to monocharged $[\text{Pt}_{26}(\text{CO})_x]^+$ oligomers (labeled up to $n = 20$).

$\text{Au}_{55}(\text{PPh}_3)_{12}\text{Cl}_6$ cluster (14 165 amu).⁴ Its formulation and its proposed two-shell Au_{55} cuboctahedral structure were based on molecular weight determinations, elemental analyses, NMR, Mössbauer spectroscopy, magnetic and conductivity measurements, and high-resolution transmission electron microscopy (HRTEM);⁴ the lack of single crystals prevented characterization by X-ray diffraction. The recent analysis of ²⁵²Cf-PD positive-ion mass spectra of several samples led to the reformulation² of this gold cluster with a Au framework patterned after the Teo cluster-of-clusters model⁵ for vertex-sharing centered icosahedra.

The above work inspired us to investigate whether ²⁵²Cf-PDMS of high-nuclearity platinum carbonyl cluster anions would provide meaningful spectral data.⁶⁻¹¹ Previous attempts to obtain FAB and laser desorption mass spectra of several triangular platinum carbonyl $[\text{Pt}_3(\text{CO})_6]_n^{2-}$ clusters ($n = 2-5$)^{12,13} had been unsuccessful. Reported herein is a preliminary account of mass spectral

(3) (a) Macfarlane, R. D. *Anal. Chem.* **1983**, *55*, 1247A. (b) Sundqvist, B.; Macfarlane, R. D. *Mass Spectrom. Rev.* **1985**, *4*, 421.

(4) (a) Schmid, G.; Pfiel, R.; Boese, F.; Bandermann, F.; Meyer, S.; Calis, G. H. M.; van der Velden, J. W. A. *Chem. Ber.* **1981**, *114*, 3634. (b) Schmid, G. *Struct. Bonding (Berlin)* **1985**, *62*, 51. (c) Schmid, G.; Klein, N. *Angew. Chem., Int. Ed. Engl.* **1986**, *25*, 922. (d) Schmid, G.; Klein, N.; Korste, L.; Kreibitz, U.; Schonauer, D. *Polyhedron* **1988**, *7*, 605. (e) Schmid, G. *Polyhedron* **1988**, *7*, 2321.

(5) (a) Teo, B. K.; Hong, M. C.; Zhang, H.; Huang, D. B. *Angew. Chem., Int. Ed. Engl.* **1987**, *26*, 897. (b) Teo, B. K.; Zhang, H. *Inorg. Chem.* **1988**, *27*, 414. (c) Teo, B. K.; Zhang, H. *Inorg. Chim. Acta* **1988**, *144*, 173. (d) Teo, B. K.; Zhang, H.; Shi, X. *Inorg. Chem.* **1990**, *29*, 2083.

(6) Spectroscopic characterization of platinum carbonyl cluster anions has previously been limited primarily to infrared analysis of the carbonyl stretching region; however, the carbonyl band shapes and frequencies often do not provide an unambiguous means either for assessing sample purity or for differentiating different platinum cluster species from one another.⁷⁻⁹ Although a comprehensive analysis of variable-temperature ¹³C and ¹⁹⁵Pt NMR spectra of several $[\text{Pt}_3(\text{CO})_6]_n^{2-}$ dianions ($n = 2-5$) was performed by Heaton and co-workers,¹⁰ ¹³C NMR spectroscopy of the closest packed platinum carbonyl clusters has not yielded meaningful data, due possibly to residual paramagnetic effects.¹¹

(7) Lewis, G. J.; Hayashi, R. K.; Dahl, L. F. *Abstracts of Papers, 195th National Meeting of the American Chemical Society and 3rd Chemical Congress of North America*, Toronto, Canada, June 1988; American Chemical Society: Washington, DC, 1988; INOR 660.

(8) The spectroelectrochemical method has recently been applied to the $[\text{Pt}_{24}(\text{CO})_{30}]^{2-}$ dianion to establish the sequences of carbonyl frequencies for seven redox-generated species.⁹

(9) Lewis, G. J.; Roth, J. D.; Montag, R. A.; Safford, L. K.; Gao, X.; Chang, S.-C.; Dahl, L. F.; Weaver, M. J. *J. Am. Chem. Soc.* **1990**, *112*, 2831.

(10) (a) Brown, C.; Heaton, B. T.; Chini, P.; Fumagalli, A.; Longoni, G. *J. Chem. Soc., Chem. Commun.* **1977**, 309. (b) Brown, C.; Heaton, B. T.; Towl, A. D. C.; Chini, P.; Fumagalli, A.; Longoni, G. *J. Organomet. Chem.* **1979**, *181*, 233.

(11) Teo, B. K.; DiSalvo, F. J.; Waszczak, J. V.; Longoni, G.; Ceriotti, A. *Inorg. Chem.* **1986**, *25*, 2262. (b) Pronk, B. J.; Brom, H. B.; de Jongh, L. J.; Longoni, G.; Ceriotti, A. *Solid State Commun.* **1986**, *59*, 349.

(12) Calabrese, J. C.; Dahl, L. F.; Chini, P.; Longoni, G.; Martinengo, S. *J. Am. Chem. Soc.* **1974**, *96*, 2614.

(13) Longoni, G.; Chini, P. *J. Am. Chem. Soc.* **1976**, *98*, 7225.

(1) (a) Texas A&M University. (b) University of Wisconsin—Madison.
(2) Fackler, J. P., Jr.; McNeal, C. J.; Winpenny, R. E. P.; Pignolet, L. H. *J. Am. Chem. Soc.* **1989**, *111*, 6434.